JOURNAL OF CATALYSIS **172,** 110–117 (1997)
ARTICLE NO. CA971861

The Catalytic Reaction of NO over Cu Supported on Meso-Carbon Microbeads of Ultrahigh Surface Area

Yun Hang Hu and Eli Ruckenstein[1]

Department of Chemical Engineering, State University of New York at Buffalo, Amherst, New York 14226

Received March 7, 1997; revised July 1, 1997; accepted August 6, 1997

The catalytic reaction of NO with meso-carbon microbeads (MCMB) of ultrahigh surface area (3187 m^2/g) in the presence of 20 wt% supported Cu was investigated. High conversions of NO were obtained at 330°C, higher by a factor of about six than those over Cu/activated carbon for the same amount of catalyst. The NO conversion decreased because of sintering with increasing decomposition temperature of MCMB impregnated with $Cu(NO_3)_2$. A mechanism for the NO + C reaction was suggested by calculating the activation energy barriers of the possible elementary steps using the bond-order conservation method. One concludes that the NO dissociation aided by C and the disproportionation of NO are the preferred pathways of the reaction.

1. INTRODUCTION

NO_x is considered an environmental hazard because it contributes to the formation of photochemical smog and acid rain. For this reason, its decomposition from combustion exhaust streams became desirable (1, 2). Although NO is thermodynamically unstable, it exhibits a high resilience to decomposition. The ammonia selective catalytic reaction process is now applied to stationary sources to decompose NO, but this process is unsuitable for small scale exhausts (3–6). In addition, this process has a number of negative features: it is expensive, ammonia "slip" is dangerous, and ammonia is corrosive. Therefore, an efficient NO_x reduction process which does not employ ammonia as reductant is needed. Hydrocarbons and carbon constitute attractive, alternative reductants to ammonia (7–12).

Over the last 30 years, considerable work has been performed in the field of the catalytic oxidation of carbon. The effects of copper, nickel, palladium, iron, and other transition metals have been studied (13, 14). However, the main oxidizing reactants have been combinations of oxygen, steam, and carbon dioxide. Shelef and Otto (15) observed a catalytic effect of the impurities present in carbon on NO reduction and suggested using transition metals as catalysts for this reaction. Watts (16) noted that the presence of copper increases the rate of carbon oxidation, and Inui *et al.* (17), combining the first series of transition metals (Ni, Fe, or Co) with lanthanum oxide and precious metals (Pt, Ru, Rh, or Pd), as well as Yamashita *et al.* (18), combining copper and nickel, have detected an increase in NO conversion. Illan-Gomez *et al.* (19), using temperature-programmed reduction (TPR), studied the effect of transition metals on the NO reduction by carbon.

In this paper, meso-carbon microbeads (MCMB) of ultrahigh surface area are used as both support for Cu and reductant of NO. A high conversion of NO with a high rate at the low temperature of 330°C was obtained over Cu/MCMB. The effect of the decomposition temperature of the Cu nitrate impregnated MCMB on the catalytic reaction between NO and C, the surface area and pore size distribution of the catalyst, the surface composition of Cu/MCMB, the surface species formed during reaction, as well as the reaction mechanism were investigated.

2. EXPERIMENTAL

2.1. Catalyst Preparation

The catalysts were prepared by impregnating the meso-carbon microbeads (MCMB) (M-30, Osaka Gas Co. LTD, Japan) and the activated carbon (AC) (Aldrich Chemicals, 20–40 mesh) with an aqueous solution of Cu nitrate (Alfa chemical) (the Cu loading was 20 wt%). This was followed by drying at room temperature in air and by decomposition at a temperature between 300 and 450°C, in He for 3 h. The samples prepared from MCMB and from AC are denoted as Cu/MCMB and Cu/AC, respectively.

2.2. Reaction

The reaction was carried out under atmospheric pressure in a vertical quartz tube (6 mm ID) reactor, in which Cu/C or C particles (weight: 0.25 g) were held on quartz wool. The feed gas had a gas hourly space velocity (GHSV) of 4800 $cm^3\,g^{-1}\,h^{-1}$ and contained 4 mol% NO (in He). The catalyst was heated to the reaction temperature in an electric furnace in a He flow. The reactant/product mixtures were analyzed with an *in-situ* gas chromatograph (model 3700, Varian) equipped with Porapak Q and 5A molecular

[1] To whom correspondence should be addressed.

0021-9517/97 $25.00

sieve columns. The selectivities of N_2 and CO_2 are defined as $N_2/(N_2+N_2O)$ and $CO_2/(CO+CO_2)$, respectively. The material balances of C, N, and O were calculated and the difference was smaller than 10%.

2.3. *BET Surface Area and Pore Size Distribution Measurements*

A Micromeritics ASAP 2000 instrument was used to determine, via nitrogen adsorption at 77 K, the surface area and the pore size distribution. The surface area was calculated by the BET method, while the pore size distribution curve was obtained from the adsorption branch of the N_2 isotherm by the BJH method. The micropore surface area was calculated from the *t*-plot. The sample was degassed at 200°C in a high vacuum before measurements.

2.4. *O_2 Chemisorption*

In order to determine the Cu surface area of Cu/C, oxygen chemisorption experiments were performed at room temperature, using a Micromeritics ASAP 2010C chemisorption instrument. The sample was subjected to the high vacuum of 10^{-5} Torr for 60 min at 300°C, before performing the O_2 chemisorption experiment. The Cu surface area of Cu/C sample was determined assuming a 1:2 (O_2:Cu) stoichiometry.

As noted in the literature (20), oxygen chemisorption is more suitable for the determination of Cu than hydrogen chemisorption, because the interactions between H_2 and Cu are very weak. In addition, while the chemisorptions have been usually carried out at 77 K, they had to be performed in the present case at room temperature, because of the microporosity of MCMB. The amount of O_2 adsorbed on pure carbon (which expressed in terms of Cu area was 0.7 m^2/g for MCMB and 0.3 m^2/g for activated carbon) was subtracted from the Cu surface areas determined for the Cu/C samples. Since oxygen may also oxidize to some extent some sublayers, the values obtained for the Cu surface area provide at least the relative sequence.

2.5. *XPS*

The XPS analysis was carried out using an SSI Model 100 small spot ESCA instrument, equipped with an AlKα monochromatized X-ray source. The binding energies were referenced to the C_{1s} level (285.0 eV). The atomic ratios were estimated from the XPS spectra after background subtraction and after correcting the relative peak areas with the corresponding atomic sensitivity factors.

3. ACTIVATION ENERGY CALCULATION

The activation energies were calculated using the Bond-order conservation Morse potential method (BOC-MP). This method was well described in the literature (21–23) and its qualitative reliability demonstrated for several reactions (24–26). The basic parameter of this approach is the maximum metal-adsorbate (M-A) two-center bond energy (Q_{0A}), which can be calculated from the experimental atomic heat of chemisorption (Q_A), using the expression (21–23)

$$Q_A = Q_{0A}(2 - 1/n),$$

where n is the coordination number of the chemisorbed atom A. The molecular chemisorption heat (Q_{AB}), when only A is coordinated to the metal atoms, can be calculated using the following expressions:

(i) weak M_n-AB bonding (close shell molecules, such as CO, NO, and CO_2)

$$Q_{AB} = Q_{0A}^2/[(Q_{0A}/n) + D_{AB}],$$

(ii) strong M_n-AB bonding (radicals that retain localized unpaired electrons such as OH, OOH, and CH_3O)

$$Q_{AB} = Q_A^2/(Q_A + D_{AB}),$$

(iii) intermediate M_n-AB bonding (the monovalent carbon radicals, such as CH_3, CH_2OH, and HCO)

$$Q_{AB} = (1/2)\{Q_{0A}^2/[(Q_{0A}/n) + D_{AB}] + Q_A^2/(Q_A + D_{AB})\}.$$

In the above expressions, Q_A is the chemisorption heat of the coordinated atom A and D_{AB} is the heat of dissociation of A-B in the gas phase.

The activation energy can be calculated using the following equations:

(i) for the $AB_{(s)} \rightarrow A_{(s)} + B_{(s)}$ reaction

$$\Delta E = (1/2)\{D_{AB} + [Q_A Q_B/(Q_A + Q_B)] + Q_{AB} - Q_A - Q_B\},$$

(ii) for the $A_{(s)} + BC_{(s)} \rightarrow [A\cdots B\cdots C] \rightarrow AB_{(s)} + C_{(s)}$ reaction

$$\Delta E = (1/2)\{D + [Q_{AB} Q_C/(Q_{AB} + Q_C)] + Q_A + Q_{BC} - Q_{AB} - Q_C\},$$

where $D = D_A + D_{BC} - D_{AB} - D_C$.

The heats of adsorption of C and O are available in Ref. (20). Because the adsorption heat of the N atom is between those of C and O, and the difference between those of C and O is small, it is reasonable to consider that the adsorption heat of N is the arithmetic average of C and O (21) (see Table 1).

TABLE 1

The Heat of Atomic Chemisorption on Cu(111) (21)

Atom	Chemisorption heat (kcal/mol)
C	120
N	111
O	103

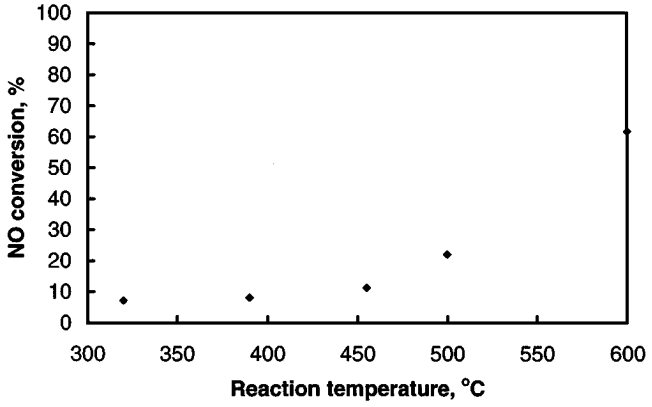

FIG. 1. The initial NO conversion vs reaction temperature over pure meso-carbon microbeads. (Feed gas: 4% NO (in He), GHSV = 4800 $cm^3 g^{-1} h^{-1}$.)

4. RESULTS

4.1. The Reaction of C with NO

Figure 1 shows that the NO conversion by the MCMB is only 22% up to 500°C, hence that the reactivity of the pure MCMB is low. In contrast, as shown in Fig. 2a, when Cu is supported on MCMB, the NO conversion over Cu/MCMB is higher. However, the conversion of NO depends on the decomposition temperature in He of the impregnated catalyst. At a reaction temperature of 330°C, the initial conversion of NO by C is 100% over the Cu/MCMB catalyst which was only dried at room temperature in air, 82% over that decomposed at 300°C, 69% over that decomposed at 380°C and 47% over the one decomposed at 450°C. However, the NO conversion decreases with reaction time, the initial decrease being more rapid over the Cu/MCMB catalyst, which was only dried, than over that decomposed at 300°C.

The selectivity to N_2 defined as $100 \times N_2/(N_2 + N_2O)\%$ also depends on the decomposition temperature of the precursor catalyst (Fig. 2b). At a reaction temperature of 330°C, the initial selectivity to N_2 is 100% over the Cu/MCMB catalyst which was only dried, 95% over that decomposed at 300°C, 85% over that decomposed at 380°C, and 77% over that decomposed at 450°C. However, the selectivity to CO_2 is almost 100% for all Cu/MCMB samples.

It is important to compare the performances of Cu/MCMB and Cu/AC. At 330°C, the initial NO conversion was 14% over Cu/AC and 82% over Cu/MCMB, indicating that the NO conversion over Cu/MCMB is 5.9 times higher than that over Cu/AC. The ratio between the two conversions is even higher after 4 h (Fig. 2a).

The rates of NO conversion and CO_2 formation are presented in Figs. 3a and b, respectively. The rate of formation of CO_2 is somewhat smaller than half the rate of NO conversion, because some N_2O is formed during the reaction (see Fig. 2b which provides information about the selectivity to N_2 defined as $100 \times N_2/(N_2 + N_2O)\%$).

4.2. The Adsorption of N_2

The adsorption of N_2 was carried out at the temperature of liquid nitrogen (−77°C) for both Cu/MCMB and Cu/AC, and the isotherms are presented in Fig. 4. As shown by Fig. 4, the isotherms for MCMB and Cu/MCMB belong to type I adsorption, for which the adsorbed volume increases at first very fast, and then remains nearly constant with increasing relative pressure of N_2. All the isotherms exhibit a very narrow hysteresis loop. Compared with the pure MCMB, the Cu/MCMB has a smaller adsorption (or desorption) volume at the same relative pressure, because the former has a much greater surface area and pore volume than the latter.

The specific surface areas, calculated by the BET method from the isotherms (Table 2), are: 3187 m^2/g for the nonheat-treated MCMB and 3211 m^2/g for the MCMB heat-treated at 300°C for 3 h, and 1314, 1276, and 1377 m^2/g for

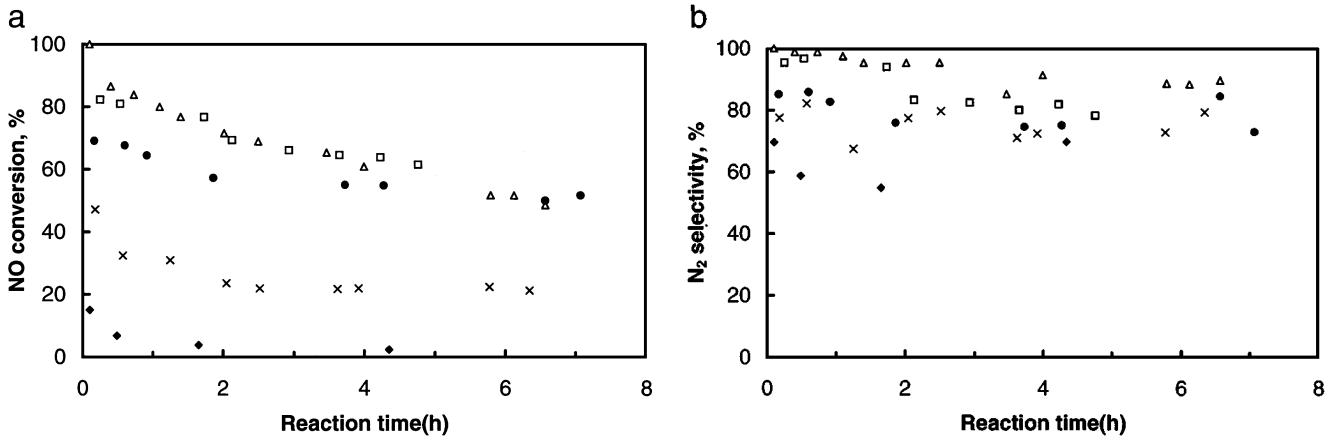

FIG. 2. The NO conversion (a) and N_2 selectivity (b) vs reaction time over Cu/meso-carbon microbeads. (Temperature: 330°C; feed gas: 4% NO (in He), GHSV = 4800 $cm^3 g^{-1} h^{-1}$; △—Cu/MCMB only dried, □—Cu/MCMB decomposed at 300°C, ●—Cu/MCMB decomposed at 380°C, ×—Cu/MCMB decomposed at 450°C, ◆—Cu/AC decomposed at 300°C.)

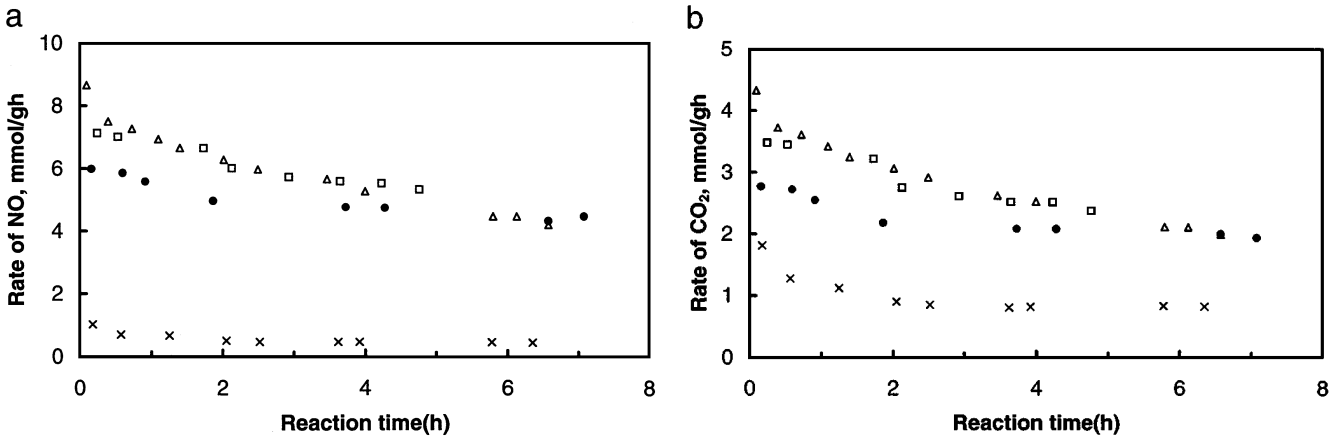

FIG. 3. Rate per gram of catalyst vs reaction time over Cu/meso-carbon microbeads (a) for NO conversion (b) for CO_2 formation. (Temperature: 330°C; feed gas: 4% NO (in He), GHSV = 4800 $cm^3\,g^{-1}\,h^{-1}$; △—Cu/MCMB only dried, □—Cu/MCMB decomposed at 300°C, ●—Cu/MCMB decomposed at 380°C, ×—Cu/MCMB decomposed at 450°C.)

Cu/MCMB decomposed at 300, 380, and 450°C for 3 h, respectively. In order to determine the ratio between the micropore surface area and the total surface area, we used the *t*-plot method and the results are listed in Table 2. Table 2 reveals that the micropore surface area represents more than 95% of the total surface area.

The mesopore size distribution was obtained using the BJH method (Fig. 5). Compared with the pure MCMB, the Cu/MCMB has a smaller pore volume. However, there is no obvious effect of the calcination temperature of Cu/MCMB on the pore size distribution in the mesopore range (2–50 nm).

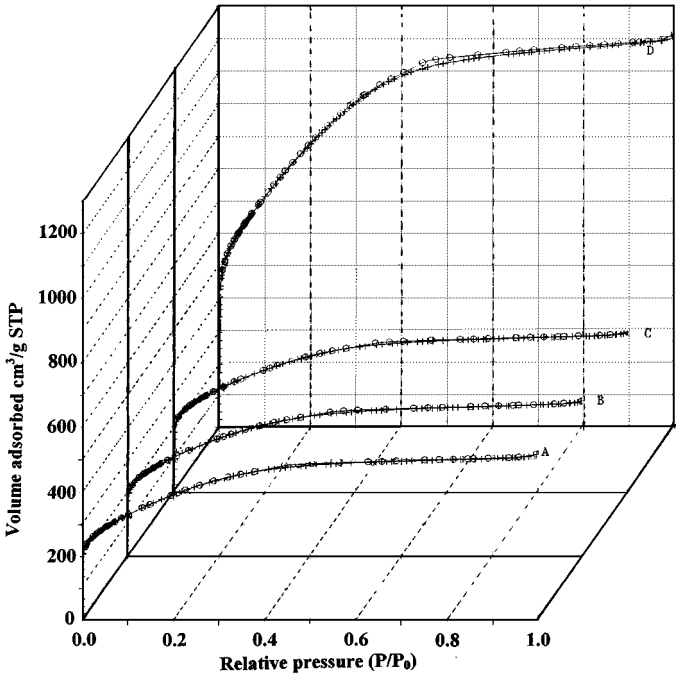

FIG. 4. Adsorption isotherms of mesocarbon-microbead and Cu/mesocarbon-microbeads (A—Cu/MCMB decomposed at 450°C, B—Cu/MCMB decomposed at 380°C, C—Cu/MCMB decomposed at 300°C, D—MCMB) (+—adsorption, ○—desorption.)

4.3. Cu Surface Area of Cu/C

Table 3 shows that the Cu surface area of Cu/MCMB samples decreases from 3.1 to 0.9 m^2/g when the decomposition temperature during the preparation process increases from 300 to 450°C. The Cu surface area of Cu/AC (7.7 m^2/g) is 2.5 times greater than that of the corresponding Cu/MCMB (both heat-treated at 300°C).

4.4 X-Ray Photoelectron Spectroscopy (XPS)

Cu, O, and C were detected in the surface layer of Cu/MCMB by XPS (Fig. 6). There are two peaks at about 932 and 935 eV which can be assigned to the Cu species (Fig. 6a); three peaks at about 285, 286, and 289 eV which can be assigned to the C species (Fig. 6b); and two peaks at about 531 and 533 eV which can be assigned to the O species (Fig. 6c).

TABLE 2

BET and *t*-Plot Surface Areas

Sample[a]	S_{micro}[b] (m^2/g)	S_{BET}[c] (m^2/g)
MCMB untreated	3030	3187
MCMB (300°C)	3051	3211
Cu/MCMB (300°C)	1260	1314
Cu/MCMB (380°C)	1225	1276
Cu/MCMB (450°C)	1322	1377
AC untreated	337	618
Cu/AC (300°C)	264	498

[a] Heated in He for 3 h at the temperature indicated.
[b] Surface area of micropores determined using the *t* plot.
[c] BET surface area.

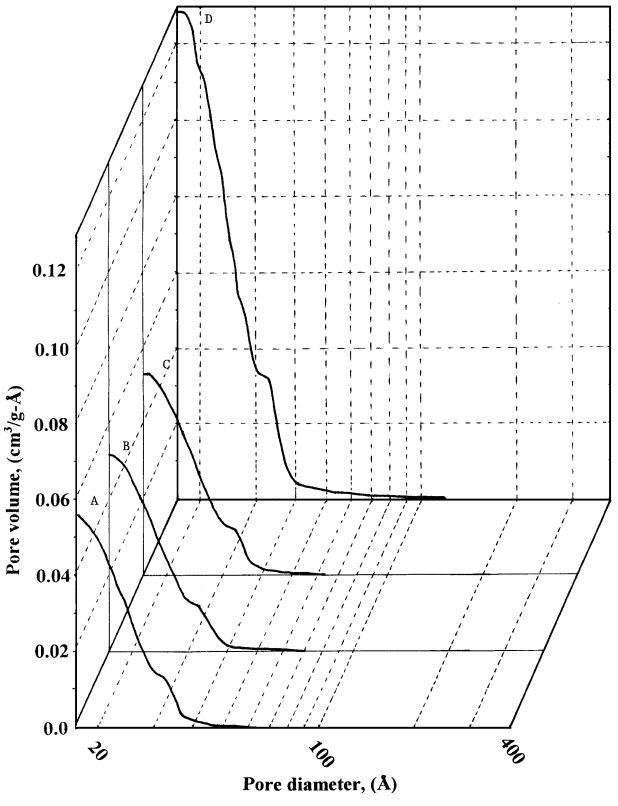

FIG. 5. The mesopore size distribution in meso-carbon microbeads and Cu/mesocarbon-microbeads. (A—Cu/MCMB decomposed at 450°C, B—Cu/MCMB decomposed at 380°C, C—Cu/MCMB decomposed at 300°C, D—MCMB.)

The surface atomic concentration of C, O, and Cu were calculated on the basis of the XPS results (Table 4). One can see from Table 4 that the concentration of Cu was 2.3 atomic% before reaction and 1 atomic% after reaction.

4.5. The Activation Energy Barriers of the Elementary Steps for NO + C Reaction over Cu(111)

We used the BOC-MP method to calculate the activation energies of all possible elementary steps of NO + C reaction over Cu(111). For N_2, NO, and CO, two kinds of adsorbed species, top and bridge, were considered. The results of the calculations are listed in Table 5 and plotted in Fig. 7.

TABLE 3

Cu Surface Area

Sample[a]	Cu surface area[b] (m^2/g)
Cu/MCMB (300°C)	3.1
Cu/MCMB (380°C)	1.6
Cu/MCMB (450°C)	0.9
Cu/AC (300°C)	7.7

[a] Treated in He for 3 h at the temperature indicated.
[b] Determined by O_2 chemisorption.

TABLE 4

XPS Determined Surface Composition of 20 wt% Cu/MCMB (Heat Treated at 300°C for 3 h)

Reaction	Cu (atm%)	C (atm%)	O (atm%)
Before	2.3	88.7	9.0
After	1.0	89.8	9.2

5. DISCUSSION

5.1 The Surface and Pore Size Distribution of Cu/MCMB

Figure 4 indicates that the adsorption isotherms of MCMB and Cu/MCMB exhibit an initial rapid increase of the amount adsorbed, followed by a long, nearly horizontal region, with increasing relative pressure. Most physisorption isotherms can be grouped into five classes (27, 28). The adsorption isotherms of MCMB and Cu/MCMB are of type I (Fig. 4), which characterizes the micropores (29). Consequently, the micropores predominate in MCMB and Cu/MCMB. Since the isotherms of MCMB and Cu/MCMB

TABLE 5

Activation Barriers for Forward (E_f) and Reverse (E_r) Elementary Reactions for $2NO + C$ to $N_2 + CO_2$ on Cu(111)

Reaction	State of adsorbed molecule	Activation energy (kcal/mol) E_f	E_r
$NO_{(s)} \rightarrow N_{(s)} + O_{(s)}$	Top	5	48
	Bridge	7	46
$NO_{(s)} + C_{(s)} \rightarrow N_{(s)} + CO_{(s)}$	Top	0	55
	Bridge	0	56
$NO_{(s)} + NO_{(s)} \rightarrow N_2O_{(s)} + O_{(s)}$	Top	0	21
	Bridge	0	17
$NO_{(s)} + N_{(s)} \rightarrow N_2O_{(s)}$	Top	16	1
	Bridge	19	1
$2N_{(s)} \rightarrow N_{2(s)}$	Top	18	37
	Bridge	17	38
$N_{2(s)} + O_{(s)} \rightarrow N_2O_{(s)}$	Top	42	0
$C_{(s)} + O_{(s)} \rightarrow CO_{(s)}$	Top	3	53
	Bridge	2	54
$CO_{(s)} + O_{(s)} \rightarrow CO_{2(s)}$	Top	0.3	14
	Bridge	2	13
$N_2O_{(s)} \rightarrow N_2O_{(g)}$	Bridge	7^a	/
$CO_{(s)} \rightarrow CO_{(g)}$	Top	16^a	/
	Bridge	18^a	/
$N_{2(s)} \rightarrow N_{2(g)}$	Top	15^a	/
	Bridge	17^a	/
$CO_{2(s)} \rightarrow CO_{2(g)}$	Bridge	5^a	/

Note. The activation energy of desorption cannot be provided by the BOC-MP method. The values in the table marked by [a] represent the heats of adsorption. Because, in general, the activation energy of adsorption is much smaller than that of desorption, one can equate the activation energy of desorption to the heat of adsorption.

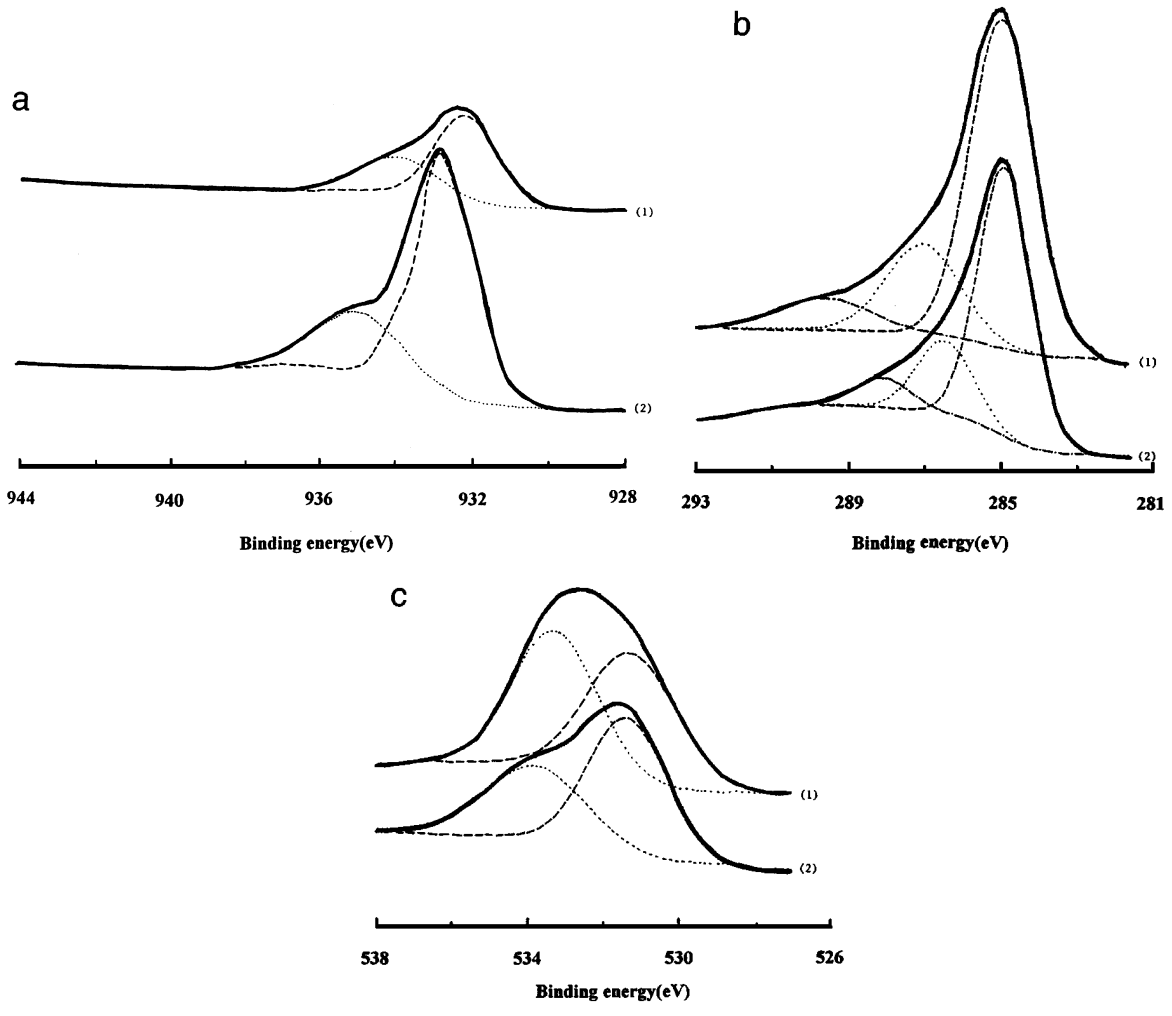

FIG. 6. The XPS spectra of Cu/MBMC prepared by decomposition at 300°C: (a) for Cu $2p_{3/2}$; (b) C_{1s}; (c) for O_{1s} (1. after reaction at 330°C for 5.5 h; 2. before reaction).

possess also a narrow hysteresis loop, which is caused by the desorption from mesopores, MCMB and Cu/MCMB contain only a small fraction of mesopores. The above conclusion is confirmed by the *t*-plot, which indicates that the micropore surface areas represent more than 95% of the total surface areas (Table 2). The pure MCMB has a surface area of 3187 m^2/g. Since each carbon atom at the surface of graphite occupies an area of 7 $Å^2$ (29), $4.56 \times 10^{22}/g$ carbon atoms are present on the surface. The total number of carbon atoms in the sample being $5 \times 10^{22}/g$, 91% of all the carbon atoms are present on the surface and are accessible to the gas. This represents an extremely open structure. After the carbon was impregnated with a $Cu(NO_3)_2$ solution and the system subjected to heating in He, the surface area decreased tremendously. Two main causes can decrease the surface area: (i) the plugging of the micropores by copper and (ii) the collapse of some pores of MCMB during the decomposition process. Since the surface area of pure MCMB did not decrease after the treatment at 300°C, it is likely that the decrease in surface areas of Cu/MCMB is mainly due to the plugging of some of the micropores by copper.

5.2. Catalytic Reaction between NO and C

There are two pathways for the reaction of C with an oxidant: one is uncatalytic, the direct reaction of NO with C; the other is catalytic, the NO reaction with C over a catalyst. The pure carbon microbeads have a very low activity, whereas the Cu/MCMB samples have high activity (Figs. 1 and 2). This indicates that, although MCMB has a very high surface area, the reaction between carbon and NO is mainly catalytic. The activity of Cu/MCMB for NO reduction decreases with increasing decomposition temperature (decomposition during the preparation of the catalyst) but the surface area of Cu/MCMB does not decrease. Consequently, the decrease in activity with increasing decomposition temperature cannot be attributed to the change in the surface area of Cu/MCMB. Since the Cu surface area of

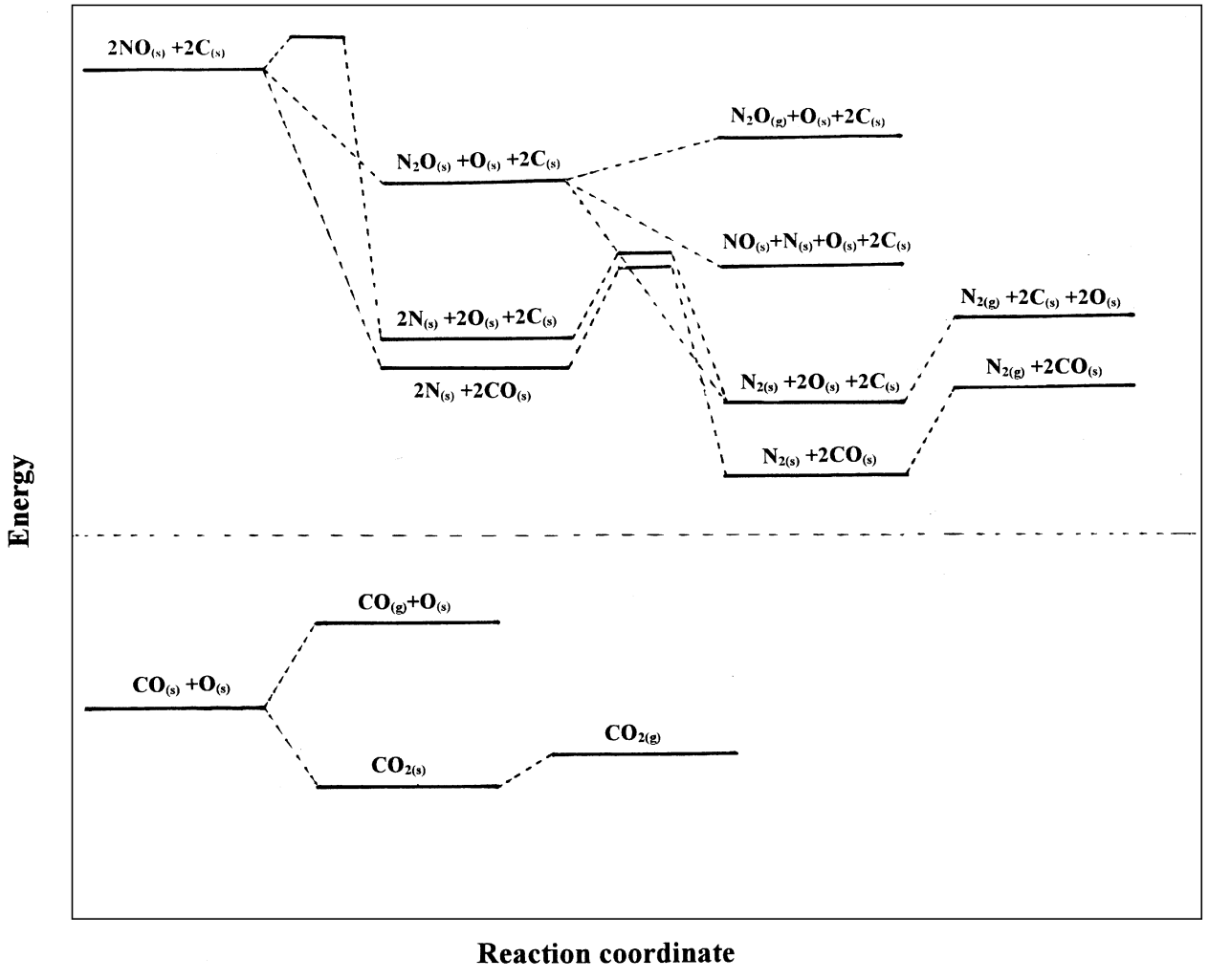

FIG. 7. Schematic energy profile for the NO + C reaction over Cu(111).

Cu/MCMB decreases with increasing decomposition temperature, the decrease in the activity of Cu/MCMB with increasing decomposition temperature is most likely due to the increased sintering of Cu. It is worth noting that, although the Cu surface area of Cu/AC is 2.5 times as large as that of the corresponding Cu/MCMB, its activity is smaller than that of Cu/MCMB. This indicates that the activity is also affected by the structure of the carbon and that the porous, loose, structure of MCMB provides a better cooperation (probably because of the higher mobility of C) between C and Cu.

5.3. The Surface Composition of Cu/MCMB

In the XPS spectra of Cu/MCMB both before and after reaction, there are two peaks at about 932 and 935 eV (Fig. 6a), which can be attributed either to Cu^0 or to Cu^+ (30). The absence of a satellite peak at about 942 eV, which is characteristic for Cu^{2+}, indicates the absence of the latter ion. The surface concentration of Cu decreases after reaction (Table 4), because of the sintering of Cu and possibly because of Cu diffusion into the C. This explains the decrease of NO conversion with reaction time. The XPS spectra also exhibit three peaks at about 285, 286, and 289 eV, which can be attributed to C_{1s} (Fig. 6b). The peak at about 285 eV is consistent with a graphitic carbon (31–34), that at about 286 eV is consistent with a carbon present as a phenolic hydroxyl moiety (33, 34), and that at about 289 eV is consistent with a carbon present in carboxyl and/or ester groups (31–34). The spectrum also contains two peaks at about 533 and 531 eV, which correspond to the O_{1s} species (Fig. 6c). The peak at 533 eV is consistent with an oxygen present in the OH groups (31, 34) and the peak at 531 eV with that present in the C=O groups (31, 34). The latter two peaks are consistent with the presence of the C_{1s} peaks near 286 eV (phenolic hydroxyl groups) and 288.8 eV (carboxyl and/or ester groups).

5.4. The Reaction Mechanism

There are only a few investigations regarding the mechanism of the reaction of NO with C over transition metals

(35). The following questions can be raised: (1) How does the adsorbed NO dissociate?; (2) What intermediate containing N is formed?; (3) Why is CO_2 preferred to CO as the product? In order to examine these issues, we use Cu(111) as a model catalyst and calculate the activation energies of the elementary steps of the reaction using the BOC-MP method (Table 5). The dissociation of the adsorbed NO can occur in three ways: (a) the direct dissociation ($NO_{(s)} \rightarrow N_{(s)} + O_{(s)}$), (b) the dissociation aided by $C_{(s)}$ ($NO_{(s)} + C_{(s)} \rightarrow N_{(s)} + CO_{(s)}$), and (c) the disproportionation reaction ($NO_{(s)} + NO_{(s)} \rightarrow N_2O_{(s)} + O_{(s)}$). The calculated activation energies indicate that the direct dissociation of NO has a higher energy barrier than the dissociation aided by $C_{(s)}$ and the disproportionation reaction; as a result the latter two pathways are the preferred ones. The subsequent reactions of the N species can follow two pathways: $N_{(s)} + N_{(s)} \rightarrow N_{2(s)}$ and $N_{(s)} + NO_{(s)} \rightarrow N_2O_{(s)}$. Since the calculated activation energies are comparable, both pathways are likely to occur. The $N_2O_{(s)}$ can further dissociate to $NO_{(s)} + N_{(s)}$ or more likely to $N_{2(s)}$ and $O_{(s)}$ (the latter almost without any energy barrier). From the above considerations one can conclude that the selectivity to N_2 is much higher than that to N_2O. This result is in agreement with experiment, which shows that the selectivity defined as $100 \times N_2/(N_2 + N_2O)\%$ is higher than 70% and can be as large as 100%.

The reaction between $O_{(s)}$ and C to $CO_{(s)}$ takes place with a low activation energy, while the activation energy for the desorption of CO is relatively high (Table 5 and Fig. 7). Compared to the desorption of $CO_{(s)}$, the reaction of $CO_{(s)}$ with $O_{(s)}$ to $CO_{2(s)}$ and the desorption of $CO_{2(s)}$ have very small energy barriers (Table 5 and Fig. 7). This is why the selectivity to CO_2 is almost 100%. The above conclusions are consistent with the experimental data which show that CO (11–20 kcal/mol) desorbs with higher difficulty that the CO_2 (6–7 kcal/mol) from Cu (36, 37).

6. CONCLUSION

Meso-carbon microbeads (MCMB) with ultrahigh surface area were used for the catalytic reduction of NO over Cu supported on MCMB. The surface area decreased tremendously during the decomposition of the copper nitrate impregnated MCMB catalyst. Cu/MCMBs at 330°C provided a NO conversion six times higher than the conventional Cu/activated carbon. While the activities of both catalysts decreased with time, their ratio became even larger.

The activation energies, calculated using the bond-order conservation method, indicate that the NO dissociation aided by C and the NO disproportionation are preferred to the direct dissociation and that the selectivity to N_2 is higher than that to N_2O. Because the CO_2 formation via CO oxidation, and its desorption have much lower activation energies than the CO desorption, the selectivity to CO_2 is high. Experiment confirms both conclusions.

REFERENCES

1. Kapteijn, F., Rodriguez-Mirasol, J., and Moulijn, J. A., *Appl. Catal. B* **9**, 25 (1996).
2. Amiridis, M. D., Zhang, T., and Farraut, R. J., *Appl. Catal. B* **10**, 203 (1996).
3. Beechman, J. W., and Hegedus, L. L., *Ind. Eng. Chem. Res.* **30**, 969 (1991).
4. Bosch, H., and Janssen, F. J. J. G., *Catal. Today* **2**, 369 (1988).
5. Ham, S. W., Choi, H., and Nam, I. S., *Catal. Today* **11**, 611 (1992).
6. Forzatti, P., and Lietti, L., *Heterogen. Catal. Rev.* **3**, 33 (1996).
7. Li, Y., Battavio, P. J., and Armor, J. N., *J. Catal.* **142**, 561 (1993).
8. Hamada, H., Kintaichi, Y., Sasaki, M., Itoh, T., and Tabata, M., *Appl. Catal.* **64**, L1 (1990).
9. Kikuchi, E., Yogo, K., Tanaka, S., and Abe, M., *Chem. Lett.* 1063 (1990).
10. Ruckenstein, E., and Hu, Y. H., *Ind. Eng. Chem. Res.* **36**, 2533 (1997).
11. Sotoodehnia-Korrani, A., and Nobe, K., *Ind. Eng. Chem. Process Des. Dev.* **9**, 455 (1970).
12. Cha, C. Y., Process for selected gas oxides removal by radio frequency catalysts, U.S. Patent 5,246,554 (1993).
13. Walker, P. L., Shelef, M., Jr., and Anderson, R. A., *Chem. Phys. Carbon* **4**, 287 (1968).
14. McKee, D. W., *Chem. Phys. Carbon* **16**, 1 (1981).
15. Shelef, M., and Otto, K., *J. Colloid Interface Sci.* **73**, 31 (1969).
16. Watts, H., *J. Chem. Soc., Faraday Trans.* **54**, 93 (1958).
17. Inui, T., Ottowa, T., and Takegami, Y., *Ind. Eng. Chem. Process Res. Dev.* **21**, 56 (1982).
18. Yamashita, H., Yamada, H., and Tomita, A., *Appl. Catal.* **78**, L1 (1991).
19. Jillan-Gomez, M., Linares-Solano, A., and Salinas-Martinez de Lecea, C., *Energy & Fuels* **9**, 976 (1995).
20. Parris, G. E., and Klier, K., *J. Catal.* **97**, 374 (1986).
21. Shustorovich, E., *Adv. Catal.* **37**, 101 (1990).
22. Shustorovich, E., *Surf. Sci. Rep.* **6**, 1 (1986).
23. Shustorovich, E., *Acc. Chem. Res.* **21**, 183 (1988).
24. Shustorovich, E., and Bell, A. T., *Surf. Sci.* **253**, 386 (1991).
25. Shustorovich, E., *Catal. Lett.* **7**, 107 (1990).
26. Sellers, H., *J. Chem. Phys.* **98**, 627 (1993).
27. Brunauer, S., Emmett, P. H., and Teller, E., *J. Amer. Chem. Soc.* **60**, 309 (1938).
28. Brunauer, S., The adsorption of gases and vapors, *in* "Physical Adsorption," Vol. 1. Oxford Univ. Press, London, 1943.
29. Gregg, S. J., and Sing, K. S. W., "Adsorption, Surface Area, and Porosity." Academic Press, London/New York, 1967.
30. Ternigan, G. G., and Somorjai, G. A., *J. Catal.* **147**, 567 (1994).
31. Garder, S. D., Singamsetty, C. S. K., Booth, G. L., He, G., and Pittman C. U., Jr., *Carbon* **33**, 587 (1995).
32. Gardner, S. D., Singamsetty, C. S. K., Wu, Z., and Pittman, C. U., Jr., *Surf. Interface Anal.* **24**, 311 (1996).
33. Wang, T., and Sherwood, P. M. A., *Chem. Mat.* **6**, 788 (1994).
34. Beamson, G., and Briggs, D., High resolution XPS of organic polymers *in* "The Science ESCA 300 Database." Wiley, Chichester, 1992.
35. Illan-Gomez, M. J., Linaeres-Solano, A., Radovic, L. R., and Salinas-Martinez de Lecea, C., *Energy & Fuels* **10**, 158 (1996).
36. Kessler, J., and Thieme, F., *Surf. Sci.* **67**, 405 (1977).
37. Rasmussen, P. B., Taylor, P. A., and Chorkendoff, I., *Surf. Sci.* **269/270**, 352 (1992).